SolarPACES 2022, 28th International Conference on Concentrating Solar Power and Chemical Energy Systems
Analysis and Simulation of CSP and Hybridized Systems
https://doi.org/10.52825/solarpaces.v1i.697

Published: 12 Feb. 2024

Techno-Economic Analysis of Central Receiver Plants According to the Optical Error of the Solar Field

Iñigo Les[1][https://orcid.org/0000-0002-0334-7945], Amaia Mutuberria[1][https://orcid.org/0000-0002-2799-029X], Ana Bernardos[1][https://orcid.org/0000-0002-6670-353X], and Marcelino Sanchez[3][https://orcid.org/0000-0001-8690-2539]

[1] CENER (National Renewable Energy Center of Spain), Spain

Abstract. Among the concentrated solar power technologies (CSP), the central receiver (CR) technology is the most promising to achieve the lowest levelized cost of energy (LCOE) and the one expected to play one of the major roles in the energetic mix in the next years. For that purpose, succesful CR projects are needed, starting by the contruction and erection of a reliable heliostat field that fulfils its design specifications. In this work, the loss of energy production and the consequently rise of LCOE is investigated as function of the optical error of the heliostats. For that, a reference CR plant is defined in which the heliostat field layout and the receiver are optimized to collect the maximum annual energy. An aiming strategy is also implemented to obtain more realistic results. For instance, for a reasonable deviation of about 40-50% compared to the optical reference error, the annual collected energy can drop to a considerable 5%.

Keywords: Heliostat field, optical error, LCOE

1. Introduction

The central receiver (CR) system technology has the most potential to achieve the lowest levelized cost of energy (LCOE) of the concentrated solar power (CSP) technologies. Its role as a dispatchable technology is crucial to achieve a net zero carbon dioxide emissions scenario in the next years. To reach more cost-effective plants and boost their competitiveness, commercial CR plants have heavily increased in size during the last years as the main strategy achieving heliostat fields that account for 50% of the total investment [1]. For this reason, any small reduction in the capital cost of the heliostat field has significant impact in the overall investment and the evident potential to reduce the LCOE, needed for further encouraging the deployment of CR plants.

The heliostat field is, together with the receiver, the pathway to collect the energy that comes from the sun. Any shortcoming that may affect these elements is usually translated into a clear loss of efficiency and, at the end, a fall in the performance of the plant. When designing a heliostat, usually, a trade-off between performance and cost is taken to find the heliostat design that achieves the minimum cost while maintaining a set of given requirements. Among others, the tracking error and the slope (surface) error are the two main indicators that determine the performance of a heliostat, whose values tend to vary from design, generally worsening, during its assembly, erection and tuning on field, which, unfortunately, ends in certain underperforming or forces the plant works out of the design point.

In this context, this work presents a techno-economic analysis of the variation that the LCEO suffers as function of the abovementioned two more important heliostat's performance indicators for a given reference plant. First section presents the simulation model and several simplifications used in this work; second and third sections bring and describe the reference plant and meteorological conditions under consideration; fourth section describes the methodology to calculate the comparison metrics; fifth section presents the results; and last section brings together the conclusions and final thoughts.

2. Simulation model

A simulation model was developed to reproduce the behaviour of the heliostat field and the receiver implemented in in-house software developed by CENER. It is based on a simplified mathematical model for the concentrator optics and the convolution error theory for the optical error. This approach has extensively used in the literature for the fast computation of the optical annual performance of CR plants. Thus, the reflected image of each heliostat is described by a circular normal distribution while considering that, both the surface and the tracking error, have nearly normal probability distributions and are statistically independent.

The power provided by a single heliostat Hel at location xyz at a time t is calculated taking into account all factors that influence his performance, i.e. the cosine factor η_{cos}, the blocking and shadowing $\eta_{b\&s}$, the atmospheric attenuation η_{atm}, the interception with the receiver η_{int} and the mirror reflectance η_{ref}.

$$P_{Hel}(t) = DNI(t) \cdot A_{Hel} \cdot \eta_{ref} \cdot \eta_{cos}(xyz,t) \cdot \eta_{b\&s}(xyz,t) \cdot \eta_{atm}(xyz,t) \cdot \eta_{int}(xyz,t) \quad (1)$$

In the calculation of the losses due to blocking and shadowing, the shadow generated by the tower has not been taken into account. The reason behind this decision is to not specifically penalize the heliostats that lie in line with the sun positions, since only 30 sun positions are simulated (see further sections), and would lead to a heliostat field with wholes. Additionally, the weight that this simplification has in the annually optical performance of the plant is neglected considering the enormous size of the solar field and the purpose of the analysis.

The typical "sigma" parameter involved in the circular normal distribution is called σ_{Tot} in this manuscript and is calculated according to the following equations, Eq. (2) and (3). It is the optical error of the heliostat under solar conditions, i.e. the beam dispersion takes into consideration both the finite size of the sun and the own optical error of the heliostat. As stated before, these formulas are only valid assuming that all individual errors follow normal distributions and are statistically independent. Hereafter, optical error is only referring to the value that σ_{Hel} takes. σ_{Sun} takes the value of 2.24 mrad according to [2].

$$\sigma_{Hel} = \sqrt{\sigma_{SD}^2 + \sigma_{Track}^2} \quad (2)$$

$$\sigma_{Tot} = \sqrt{(2\,\sigma_{Hel})^2 + \sigma_{Sun}^2} \quad (3)$$

The optical error σ_{Hel} is the addition of the surface error σ_{SD}, understood as the difference between the design shape of the concentrator and the actual one, and the tracking error σ_{Track}, defined as the alignment error of the concentrator normal vector to focus the beam spot into the set point. To avoid confusions, note that the heliostat optical error σ_{Hel} is defined respect to the normal vector while the total error σ_{Sun} (under solar conditions) is respect to the reflected one. Specularity errors and surface error changes due to gravity, wind and temperature are neglected.

3. Location and DNI data

The plant is located in Maria Elena (Chile), a suitable location for the deployment of CR plants, very close to where the Cerro Dominador plant was built and started operation in 2021.

The direct normal irradiance (DNI) data have been taken from a previous publication [3]. In that work, the hourly DNI values of the typical meteorological year have been condensed in several sun positions using a sky discretization method [4]. This method is based on a roughly uniform discretization of the sky hemisphere, a subsequent triangulation of the resulting nodes and a pre-selection of the relevant triangle patches, according to the sun's annual path at a given site.

At the end (removing the positions with zero value), the set of solar coordinates and corresponding cumulative annual DNI is reduced to 30 sun positions, which are used to calculate the annual solar field performance, metric that is further used for the comparison.

4. Reference plant

The reference plant used for the analysis follows what is called the-state-of-the-art CR plant: two-tank molten salt storage system with large capacity (≥12 h) and maximum outlet temperature of 550 °C, solar field with large heliostats, cylindrical receiver made by tubes and ≥100 MW_e water/steam Rankine cycle with wet cooling system.

The heliostat field is made by 7'800 individual heliostats leading to an overall reflecting surface around 1'400'000 m^2. The heliostats have been reduced to a single spherical facet with a square aperture area of 180 m^2. The radius of the sphere of each heliostat corresponds to the slant range, i.e. the distance from the heliostat to the closest point on the equatorial plane on the receiver.

The optical error σ_{Hel} of the heliostats has been set in 1.581 mrad, an ordinary value, which actually could be too small for large heliostats according to authors' experience. Given this value and the expected size of the solar field, i.e. the last rows of heliostats should be placed about 1'600-1'800 m far from the tower. Initially and only for the optimization of the heliostat field layout (see next section), the dimensions of the receiver have been selected so that these last heliostats reflects the sun hitting the receiver surface without spillage (the 99.9% of the energy lies within the receiver). This means diameter and height equal to 18 m.

4.1 Heliostat field layout

The positions of the heliostats have been optimized to find the "optimal solar field", meaning that is the field with better objective function. The literature is considerable vast optimizing the layout of the heliostat fields. In this work, it has been followed the same approach that the one presented in [3]. The "optimal solar field" means the solar field layout which fits design specifications, in this case limited by the number of heliostats (7'800), and allows collecting the maximum energy at the minimum solar field cost.

Hence, the optimization function OF is calculated as:

$$OF = \frac{\eta_y}{k\frac{A_{field}}{N_h A_h}+1} \tag{4}$$

where η_y is the yearly efficiency of the field, N_h the total number of heliostats, A_h the heliostats area, A_{field} is the total ground area of the field and k is the division between the cost per squared meter of land and the cost per squared meter of heliostat surface.

For a given value of the parameter k, the optimal solar field is obtained by maximizing the objective function OF according to the following procedure, broadly explained (find the complete details in [3]):

1. Generate an oversized solar field according to the DELSOL layout generation algorithm [5]. This algorithm generates regular radial staggered layouts arranged in different zones according to radial and azimuthal directions forming circular sectors and is considered the-state-of-the-art in layout generation algorithms. The minimum radius of the first row has been set as 150 m, a reasonable distance in line with the literature, which usually takes the value of 0.7-0.8 times the height of the tower.
2. Calculate the annual energy provided by each heliostat.
3. Rate and sort in decreasing order the heliostats according to a new indicator based on the previously calculated annual energy, the distance to the tower and a dimensionless parameter. This helps to obtain more regular and smoother heliostat fields which further reduces the objective function OF.
4. Select the first 7’800 heliostats.
5. Calculate the value of the objective function OF.

For this work, the parameter k takes the value of 0.02, which, from the authors‘ previous experiences, leads to compress (and more realistic) heliostat fields, while practically maintaning the same annual performance. Fig. 1 shows the resulting solar field.

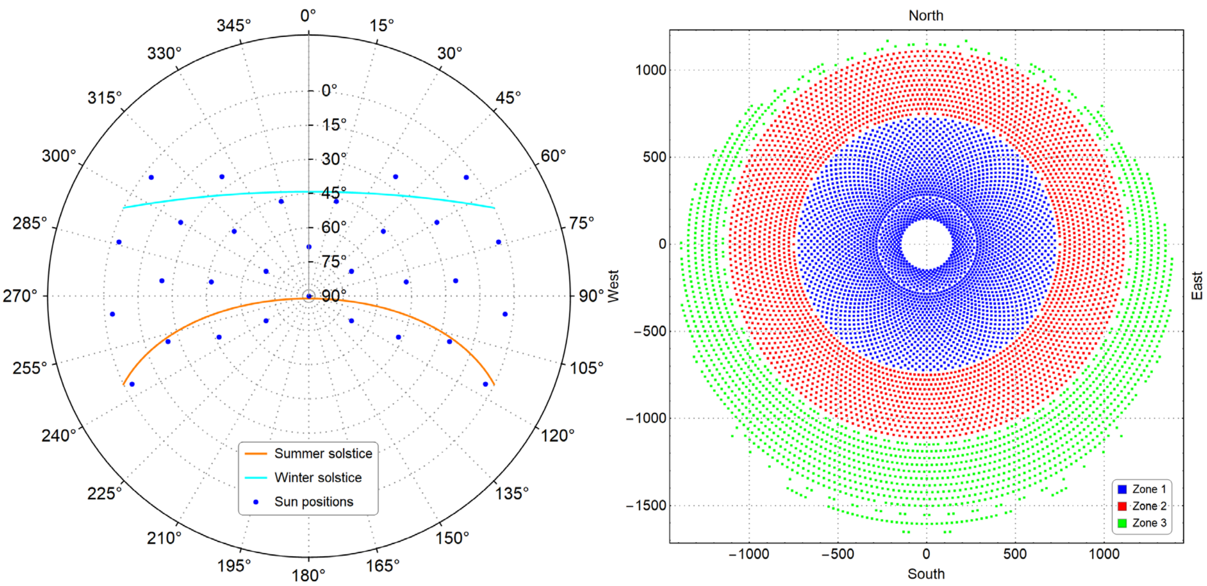

Figure 1. (Left) Sun position taken from [3]. (Right) Layout of the heliostat field of the reference plant.

4.2 Aiming strategy

The cumulative effect of thousands of energy spots reflected by the heliostats on the same part of the receiver surface can generate high peak fluxes that cause excessive thermal stress and the accelerated degradation of the receiver, which, in the worst case scenario, may end in irreversible damages and its failure. For this reason, an aiming strategy spreading the thermal power along the receiver and homogenizing the flux distribution is required to control peak thermal stress.

In this study, a methodology to distribute the energy across the receiver is also needed, otherwise the results obtained would not be realistic, i.e. would only be based on the losses by spillage and hence, the distant heliostats, but not on the whole heliostat field and how they work all together to get homogenous and practical solar flux distributions.

For that, the methodology to calculate the aim points of a solar field for a given CR plant and solar conditions (sun position, DNI, etc.) is inspired by the work presented in [6]. As summary, the approach is to drift the heliostat aim point away from the receiver equator in a vertical direction (up and down in alternative heliostat rows) along the cylinder surface, without modifying its azimuth. For that, the heliostat field is divided in three zones (see Fig. 1), the length of the drift applied to each heliostat depends on the radius of the reflected energy spot and on a parameter that is unique for each zone. Obviously, the flux map generated by each heliostat needs to be pre calculated in advance. The current implementation also includes the possibility to defocus heliostats which helps to find a more suitable solution in high DNI sun positions. In this way, the aiming strategy is determined only with four parameters (one for each zone and one for the defocus of heliostats).

4.3 Receiver

The initial size of the receiver (diameter and height equal to 18 m) is a reasonable approach if no aiming strategy is considered. In this study, implementing an aiming strategy that distributes the power along the receiver surface is mandatory to achieve comparable results. Otherwise, any increase in the optical error of the solar field may be blurred when interacting with the receiver. Consequently, the dimensions of the receiver must be optimized for the given solar field.

To this end, the diameter and the height of the receiver have been optimized according to an energetic criterion to maximize the energy arriving at the receiver less the thermal lose. To calculate the thermal loses according to the size of the receiver, a classical macroscopic approach has been followed. It has been assumed that the thermal losses are the contribution of radiation and convection. Several more assumptions have been established: the mean temperature of the receiver is 427.5 °C, the ambient temperature is 25 °C, the emissivity of the receiver surface is 0.86 and the convection coefficient is 10 W/(m2 K). With all of this in mind, the thermal losses per square meter of receiver surfaces lie in 15.4 kW/m2.

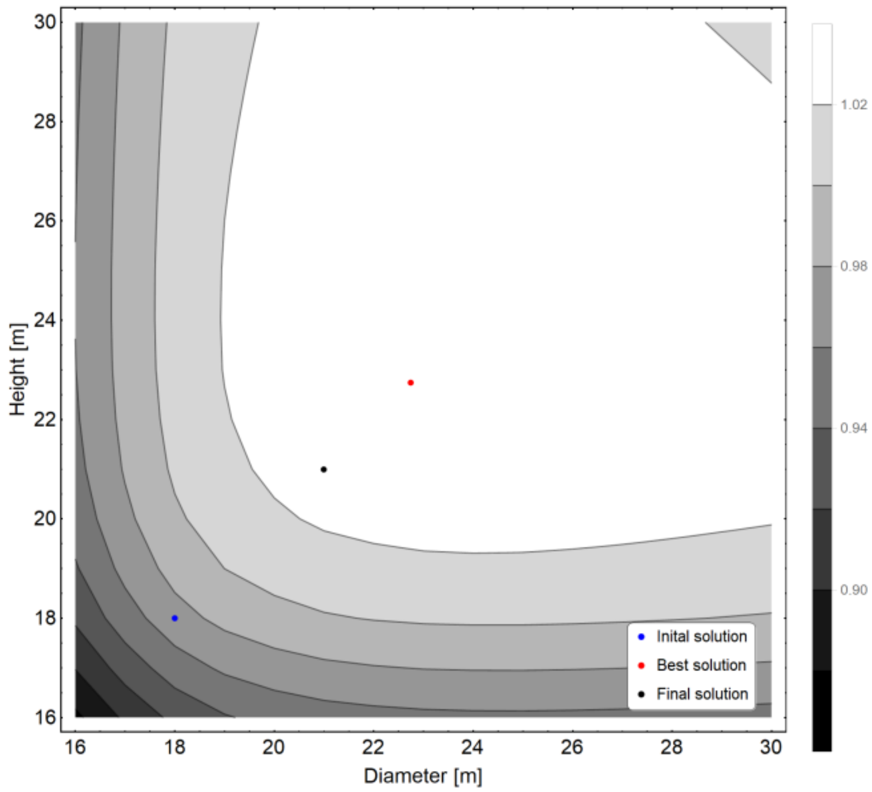

Figure 2. Contour plot of the optimization function as function of the diameter and height of the receiver.

Figure 2 shows a contour plot of the value of the optimization function as function of the values of the diameter and height relative to the initial solution, i.e. the one corresponding to diameter and height equal to 18 m. The solution that achieves the best value is diameter 22.7 m and height 22.7 m. However and considering how flat the function looks, if techno-economic reasons were included, the solution would stick in an intermediate point between the best and the initial solution. For that reason, the dimensions used further in the analysis are diameter and height equal to 21 m. Next table summarizes all required features of the reference plant as well as other relevant environmental conditions considered for the simulation.

Table 1. Centered table captions should be placed above the tables.

Location	
Latitude	-22.17°
Longitude	-69.42°
Altitude	1’500 m
Solar field	
Number of heliostats	7’800
Shape	Single spherical square facet
Aperture area	180 m^2
Radius	Two times the slant range
Optical error σ_{Hel}	1.581 mrad
Reflectance	0.94
Radius of the first row	150 m
Receiver	
Diameter	21 m
Height	21 m
Elevation	230 m
Maximum allowed flux	1.2 MW/m^2
Environmental conditions	
Atmospheric attenuation model	Mirval [7]
σ_{Sun}	2.24 mrad

5. Methodology

The financial model to calculate the LCOE and the calculations to obtain the annual performance of the plant are explained in this section.

Given a particular optical error value of the heliostats, firstly, the annually energy arriving at the receiver provided by the heliostat field is calculated through the 30 sun positions that condense the TMY. For each sun position, the aiming strategy is optimized to find the strategy (the value of the parameters that determine the aim points) that maximizes the power at the receiver for the given maximum allowed flux, which, in this case, is 1.2 MW/m^2. Since there is not a representative DNI value with whom run the simulation (remember that the TMY is condensed), the clear sky model explained in [8], taken the Linke turbidity from the SoDa database [9], the location of the plant and the sun position, is used to calculate the DNI value. This results in the optical efficiency of the solar field which is used to calculate the annual energy contribution of that sun position for the accumulated DNI. Later, the annually accumulated energy at the heat transfer fluid by the receiver is multiplied by a constant factor accounting for the rest of elements and subsystems downstream, i.e. the balance of plant (BoP), so that the annually generated electricity is calculated.

The LCOE is an important metric which provides one way to compare the economic competitiveness of different systems and scenarios. As described in Eq. (5), LCOE is typically calculated through the capital expenditure (CAPEX), the discounted operating expenditure (OPEX) and the discounted energy production. Considering that the energy production and the OPEX are independent with time, the equation is reduced to Eq (6). The results are presented in relative values to the reference plant, so there is no need to provide values to the CAPEX, OPEX and discount rate.

The levelized cost of the energy or heat (LCOH) is also an alternative metric that could have been used for the comparison. However, in this case is irrelevant as both metrics would lead to the same results.

$$LCOE = \frac{CAPEX + \sum_{t=1}^{N} \frac{OPEX_t}{(1+i)^t}}{\sum_{t=1}^{N} \frac{Production_t}{(1+i)^t}} \tag{5}$$

$$LCOE = \frac{CAPEX \cdot C + OPEX}{Production} \tag{6}$$

6. Results

Next figure shows the evolution of the annually energy arriving at the receiver and the LCOE as function of the optical error, all of them in relative values respect to the reference plant. When the optical error increases, the reflected spots of the heliostats become bigger leading to more losses by spillage. At the end, this reduces the collected energy by the receiver and, thus, negatively triggers the LCOE. For instance, for a reasonable deviation of about 40-50% compared to the optical reference error, the annual collected energy can drop to a considerable 5%. On the other hand, if a better quality solar field is achieved, the collected energy does not increase drastically, as expected (the receiver would be oversized), but would allow other profits, the reduction on the size and cost of the receiver and the easing of the operation managing the aim points are some examples.

This results, while the plant's typology, breakdown of costs and design philosophy remain equal, could be extrapolated to other plants independently of their location and size with high confident.

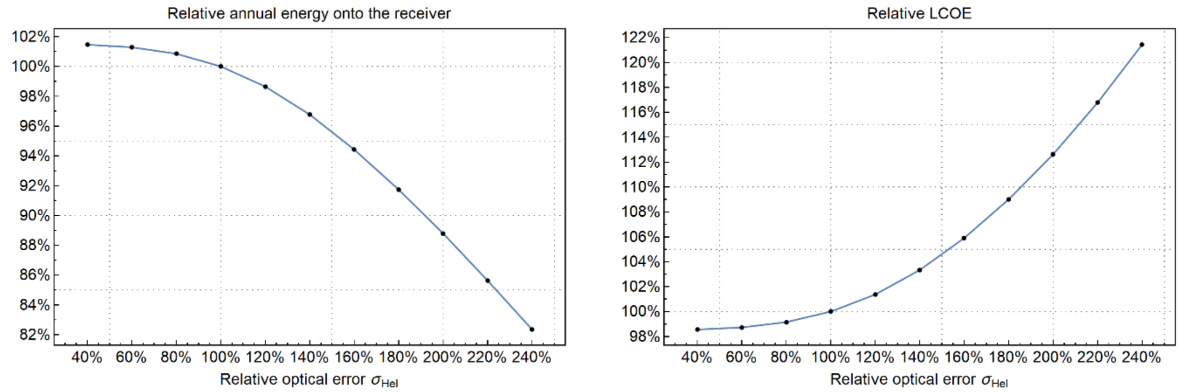

Figure 3. Evolution of the relative annual energy reaching the receiver (left) and the relative LCOE (right) depending on the relative optical error σ_{Hel} of the heliostats.

7. Conclusions

Dispatchable CSP technologies, and primarily the CR plants, are undeniably going to play a major role in the energetic mix from now on and in the next years as a complement of other forms of renewable energy. Successful projects are needed more than ever to create confident, sow good precedents and path the way to a massive implementation. Projects that struggle in their implementation and construction, specifically issues related to the solar field, and may not reach the design specifications heavily harm the confident in the technology. To avoid it, more measurements and control procedures that track deviations and check quality of the heliostats during assembly and erection on field should be a priority. More advanced calibration systems to increase tracking accuracy and innovative characterization systems to diagnose optical quality of the heliostats' concentrator are examples of expected innovations that would help in these terms. Otherwise, any deviation in the optical quality of the solar field may become a relevant underperforming of the plant and a cumbersome issue highly difficult to handle afterwards, as has been stated in this work.

Data availability statement

Data supporting the results is not available.

Author contributions

Iñigo Les is the main author leading the work and responsible of the investigation, software development, formal analysis, methodology and writing – original draft. Amaia Mutuberria also contributes in the software development, supervision and writing – review & editing. Ana Bernardos and Marcelino Sanchez take the role of the supervision and writing – review & editing.

Competing interests

Authors have no conflicts of interest to declare that are relevant to the content of this article.

References

1. A. A. Rizvi, et al. "A review and classification of layouts and optimization techniques used in design of heliostat fields in solar central receiver systems". Solar Energy, 218, 296-311, April 2021, doi: https://doi.org/10.1016/j.solener.2021.02.011.
2. M. Röger, "SolarPACES Guideline for heliostat performance testing", draft version 0.991. August, 2018.
3. E. Leonardi, et al. "Techno-economic heliostat field optimization: Comparative analysis of different layouts". Solar Energy, 180, 601-607, March 2019, doi: https://doi.org/10.1016/j.solener.2019.01.053.
4. P. Schöttl, et al., "Novel sky discretization method for optical annual assessment of solar tower plants". Solar Energy, 138, 36-46, November 2016, doi: https://doi.org/10.1016/j.solener.2016.08.049.
5. F. W. Lipps and L. L. Vant-Hull, "Programmer's manual for the University of Houston computer code RCELL: cellwise optimization for the solar central receiver project" (No. DOE/SF/10763-T5; SAN-0763-1). Houston Univ., TX (USA). Energy Lab. 1980.
6. F. J. Collado and J. Guallar, "A two-parameter aiming strategy to reduce and flatten the flux map in solar power tower plants". Solar Energy, 188, 185-189, August 2019, doi: https://doi.org/10.1016/j.solener.2019.06.001.
7. P. L. Leary and J. D. Hankins, "User's guide for MIRVAL: a computer code for comparing designs of heliostat-receiver optics for central receiver solar power plants", No. SAND-77-8280). Sandia National Lab.(SNL-CA), Livermore, CA (United States), 1979.
8. P. Ineichen and R. Perez, "A New airmass independent formulation for the Linke turbidity coefficient". Solar Energy, vol 73, pp. 151-157, September 2002, doi: https://doi.org/10.1016/S0038-092X(02)00045-2.
9. Solar radiation data http://www.soda-is.com/eng/services/climat_free_eng.php#c5.